Electronic Supplementary Material (ESI) for Journal of Materials Chemistry A.
This journal is © The Royal Society of Chemistry 2023

Highly reversible, dendrite-free and low polarization Zn metal anodes enabled by a thin SnO_2 layer for aqueous Zn-ion batteries

Yuejuan Zhang,[a,b] Penghui Chen,[a,b] Mingming Li,[a,b] Shaoqing Li,[a,b] Ying Yue,[a,b] Yanchun Wang,[a,d] Sishen Xie,[a-d] Weiya Zhou[a-d] *

[a]Beijing National Laboratory for Condensed Matter Physics, and Institute of Physics, Chinese Academy of Sciences, Beijing, 100190, China.

[b]School of Physical Sciences, and College of Materials Science and Opto-Electronic Technology, University of Chinese Academy of Sciences, Beijing, 100049, China.

[c]Songshan Lake Materials Laboratory, Dongguan, Guangdong, 523808, China.

[d]Beijing Key Laboratory for Advanced Functional Materials and Structure Research, Beijing, 100190, China.

* Corresponding Authors.

E-mail: wyzhou@iphy.ac.cn

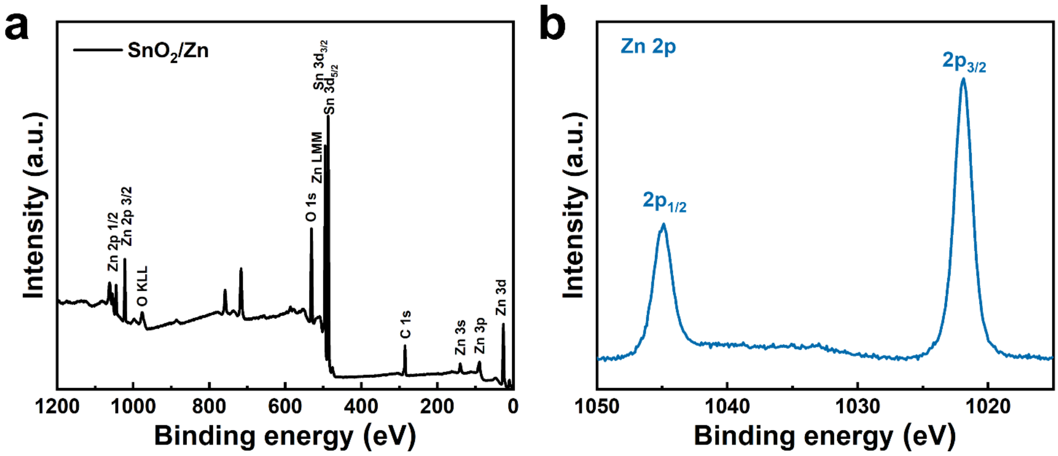

Fig. S1. (a) XPS survey spectrum of the SnO_2/Zn electrode and (b) the high-resolution scan of Zn 2p.

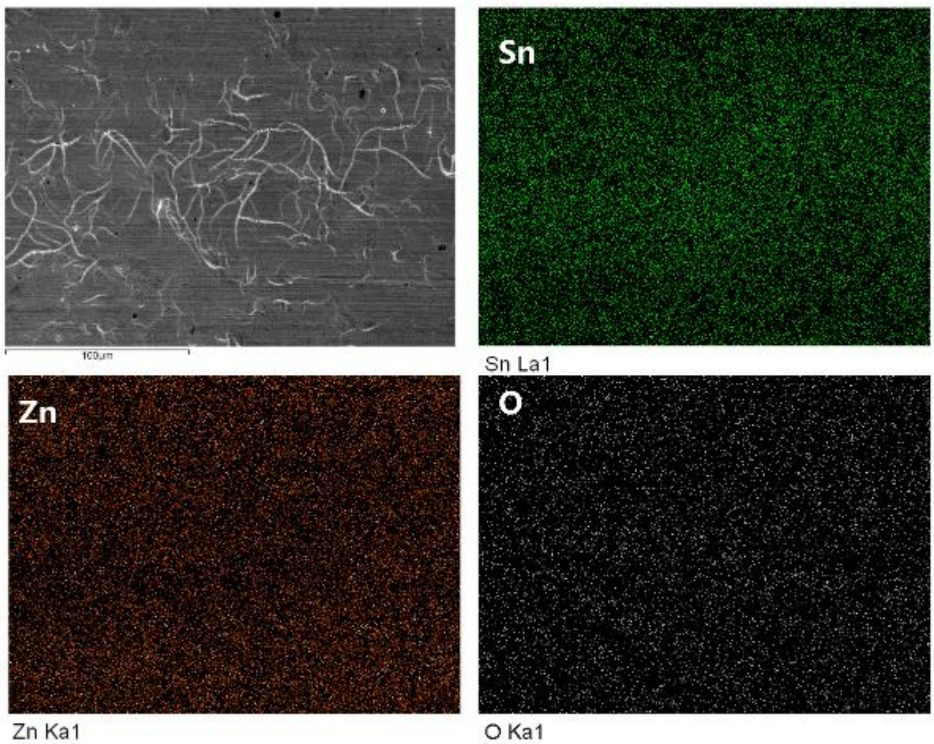

Fig. S2. SEM image and elemental mappings of the SnO_2/Zn electrode

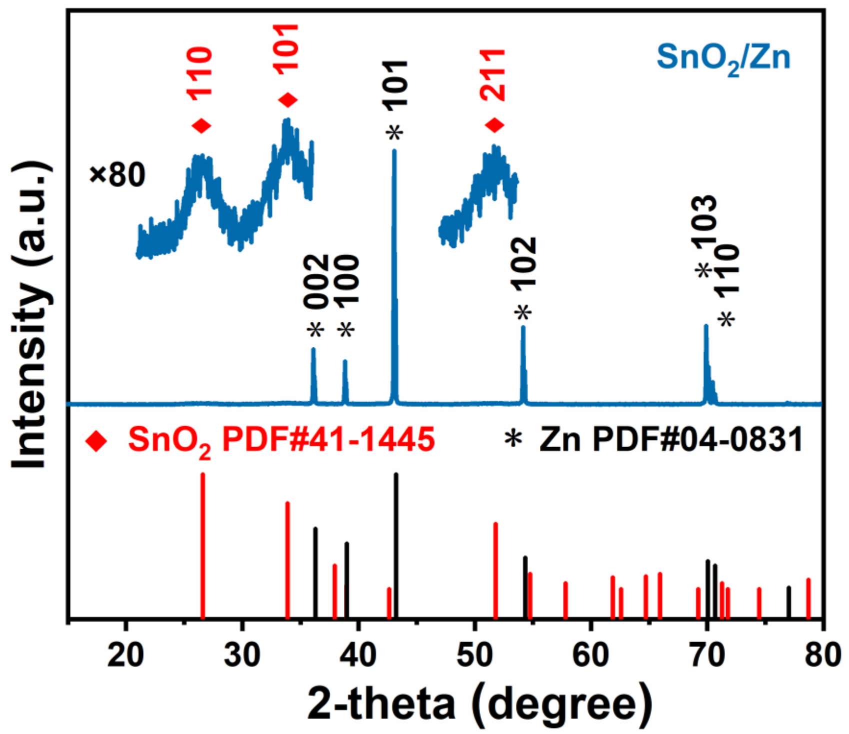

Fig. S3. GIXRD patterns of the SnO_2/Zn electrode

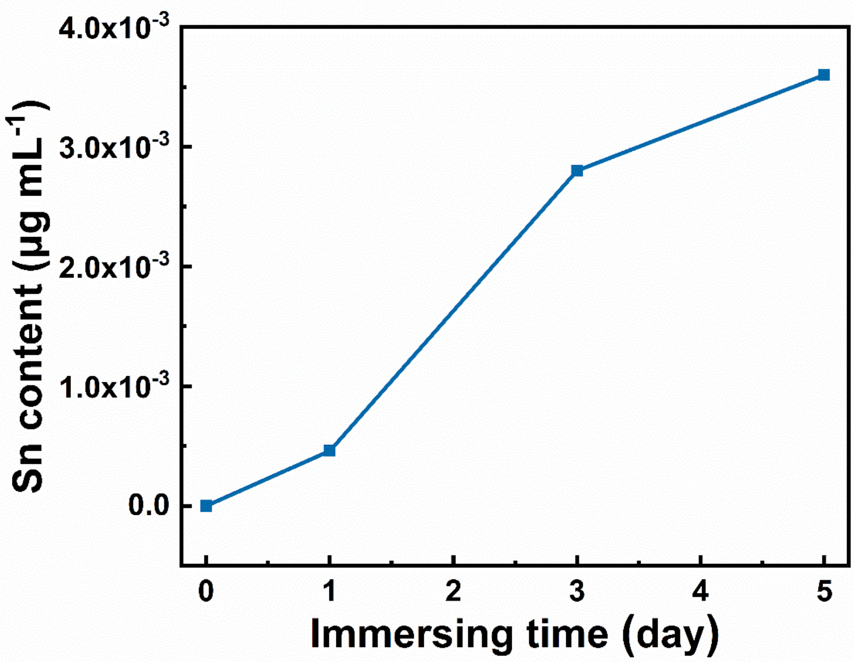

Fig. S4. The Sn content in the 2 M $ZnSO_4$ electrolyte (5 mL) after immersing SnO_2/Zn electrodes (Φ 12 mm, 5 disks) for different times

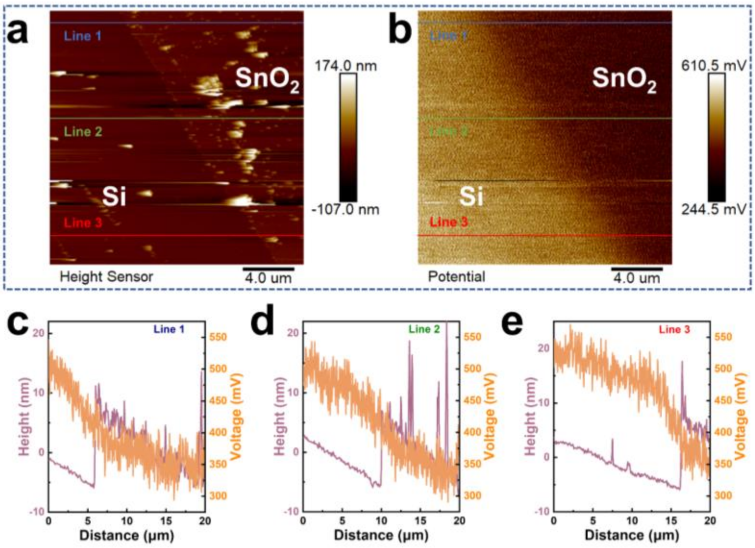

Fig. S5. (a) AFM topography image and (b) the corresponding surface potential of SnO_2/Si. (c-e) The cross-section line profiles indicated in (a, b).

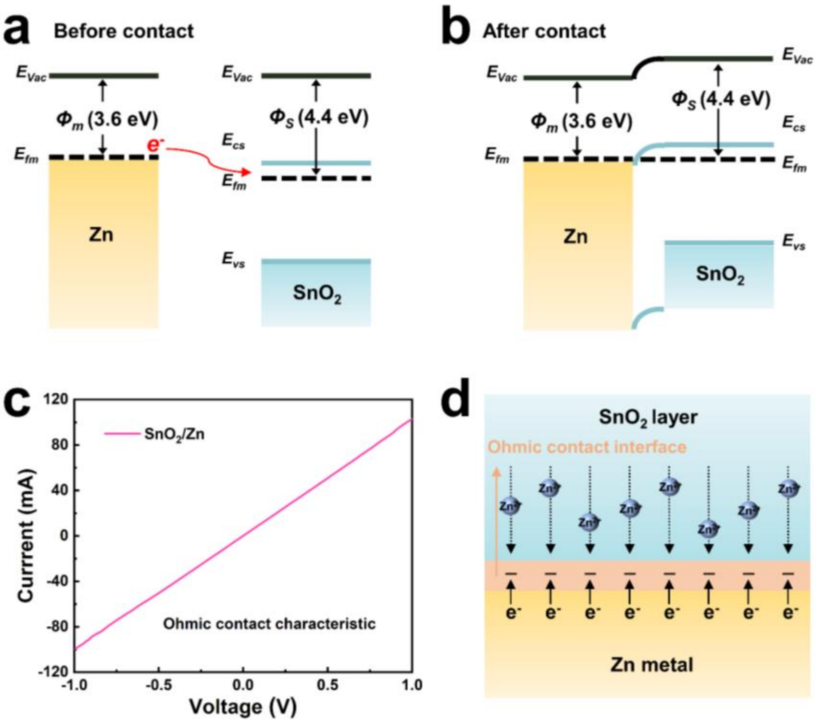

Fig. S6. The band structure of Zn metal and n-type semiconductor SnO_2 (a) before and (b) after contact. (c) The I-V curve of the SnO_2/Zn electrode. (d) A schematic illustration for the formation of an ohmic contact interface between SnO_2 and Zn metal and the resulting electron-rich region inducing rapid and uniform Zn^{2+} transport inward.

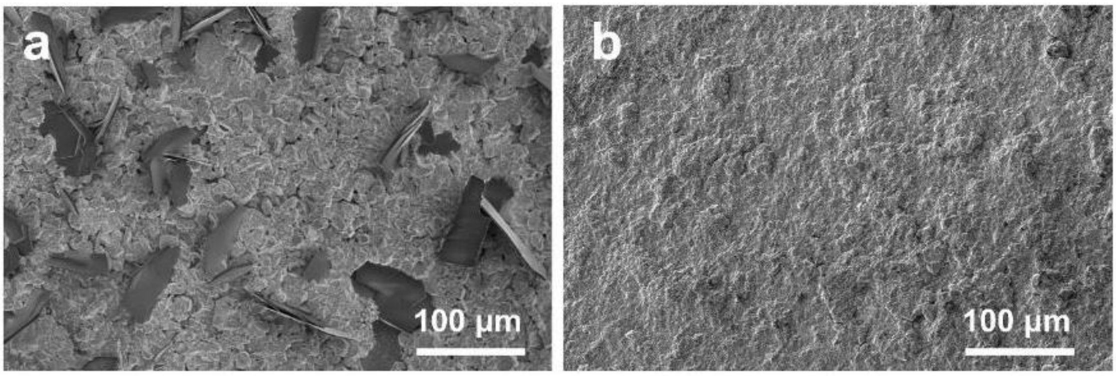

Fig. S7. SEM images of electrode surface of (a) bare Zn and (b) SnO_2/Zn after plating Zn at 10 mA cm^{-2} and 10 mAh cm^{-2}.

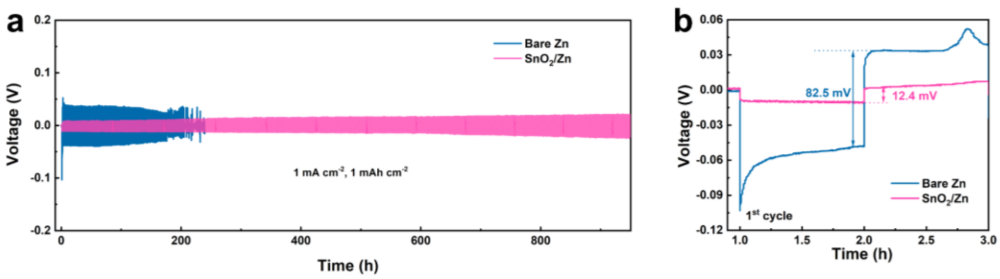

Fig. S8. (a) Long-term galvanostatic cycling of symmetric cells and (b) the corresponding time-voltage profiles with bare Zn and SnO_2/Zn electrodes at 1 mA cm^{-2}.

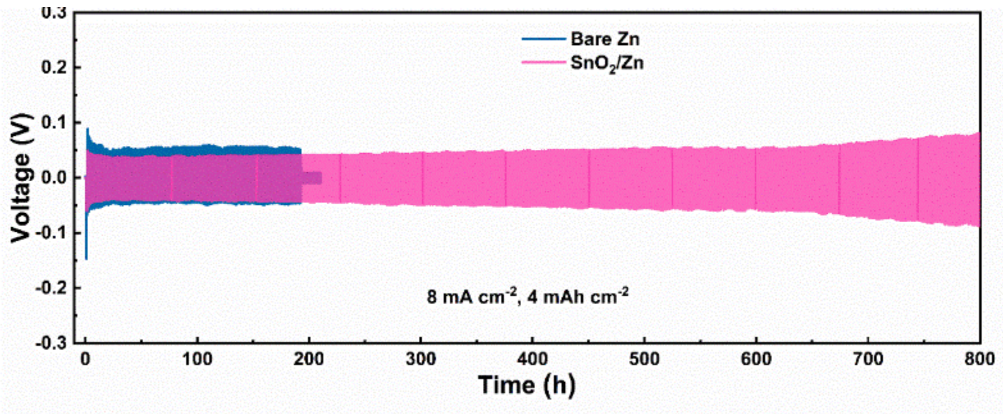

Fig. S9. Cycling performance of symmetries cells with bare Zn and SnO_2/Zn electrodes at 8 mA cm^{-2} and 4 mAh cm^{-2}

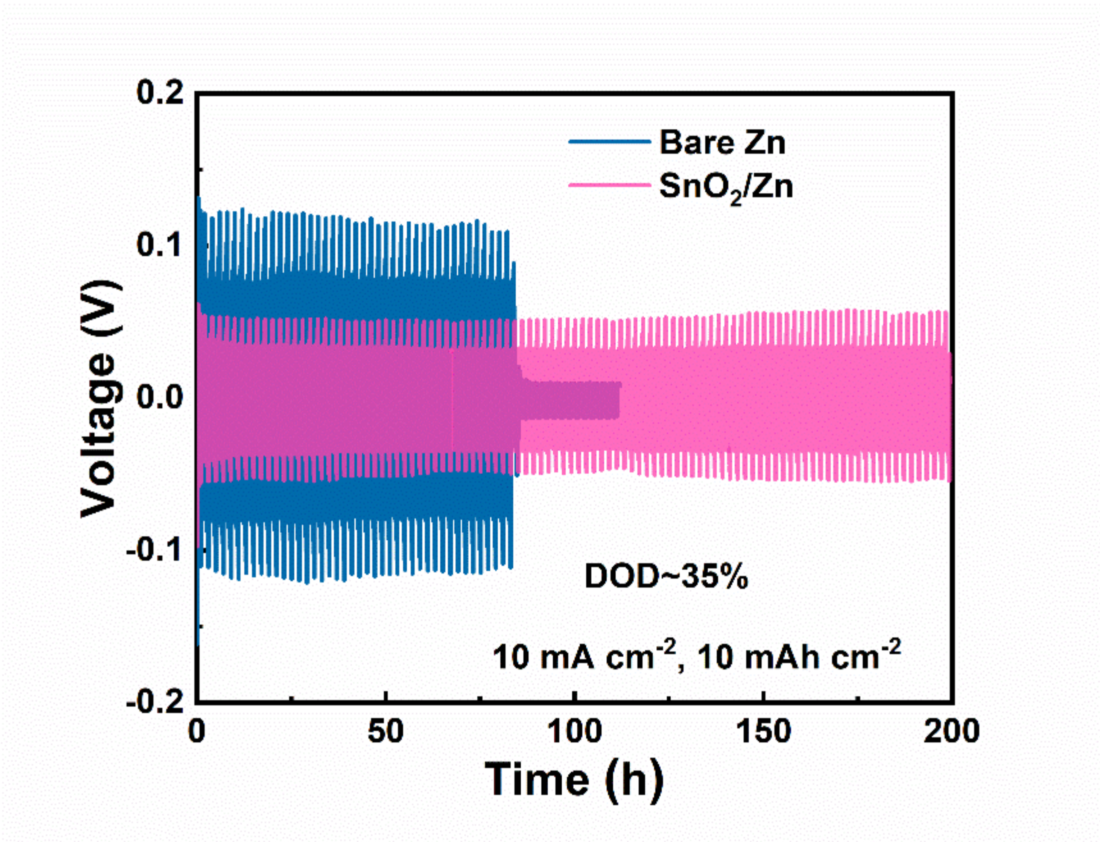

Fig. S10. Cycling performance of symmetries cells with bare Zn and SnO_2/Zn electrodes at 10 mA cm^{-2} and 10 mAh cm^{-2} (depth of discharge of ~ 35%)

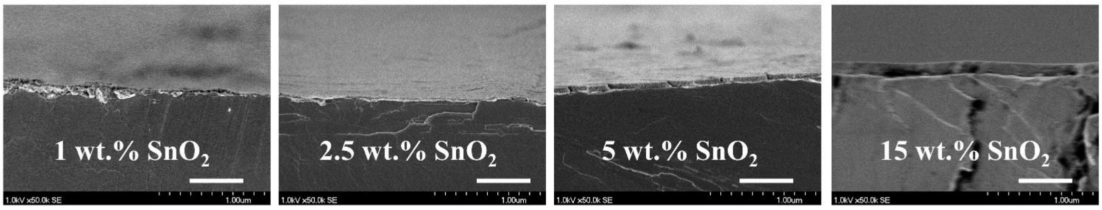

Fig. S11. Cross-sectional SEM images of SnO_2/Zn electrodes prepared with different concentrations of SnO_2 solution. Scale bar: 500 nm.

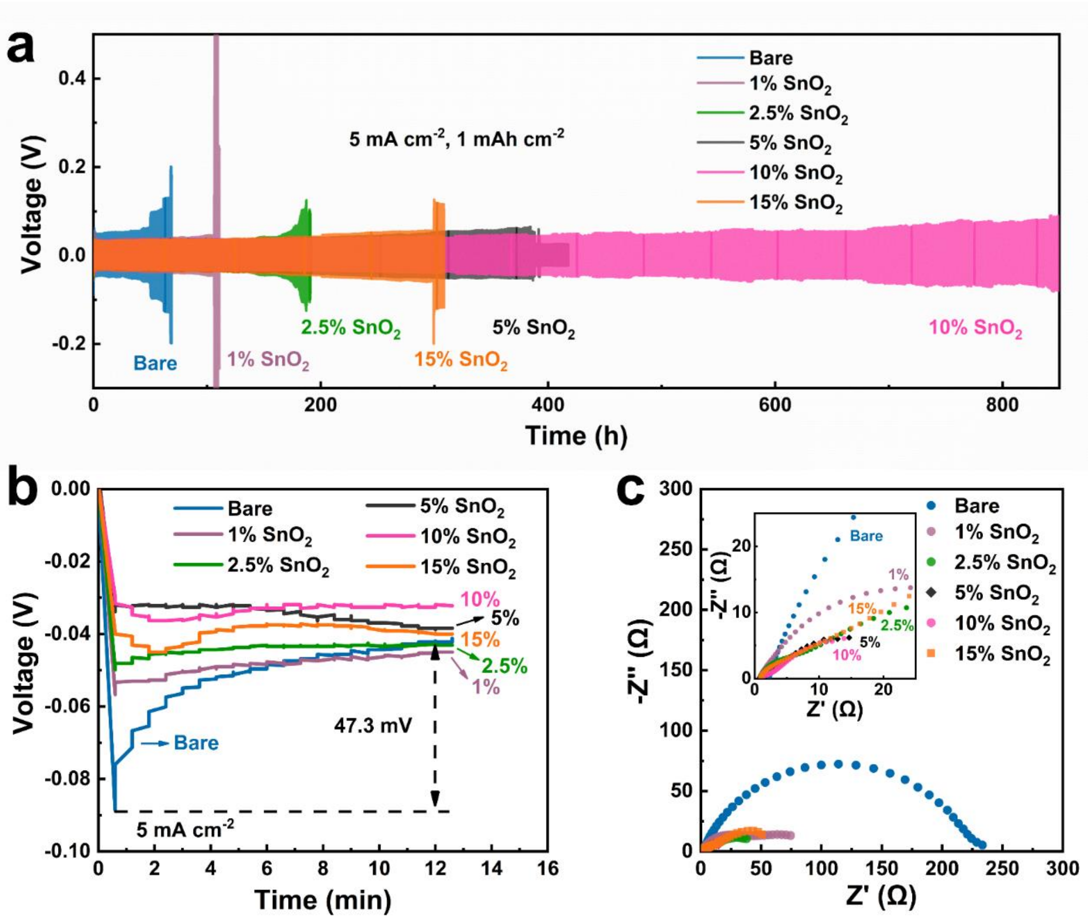

Fig. S12. (a) Galvanostatic cycling of symmetric cells and (b) the corresponding nucleation overpotentials based on the Zn anodes without and with SnO_2 layers. (c) EIS spectra (Nyquist plots) of Zn symmetrical cells without and with SnO_2 layers.

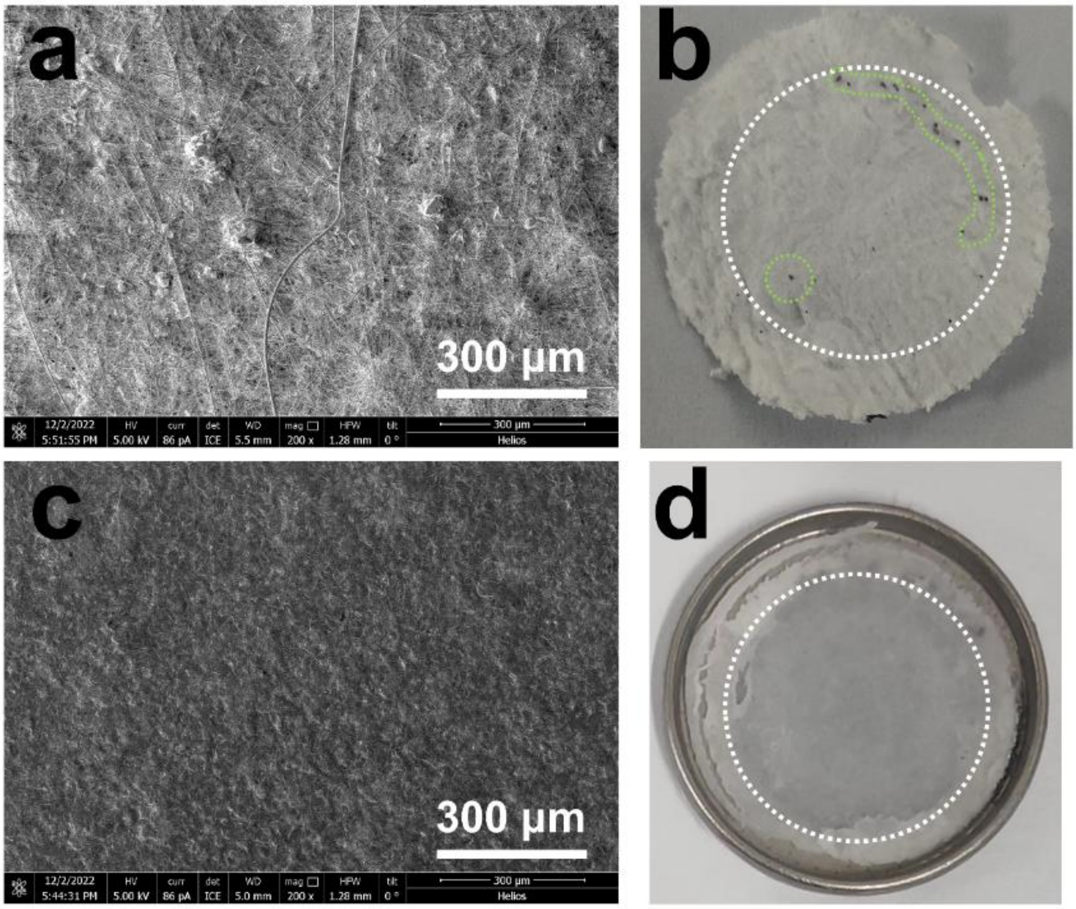

Fig. S13. (a) SEM image of 1% SnO_2/Zn anode surface after 415 cycles and (b) the corresponding photos of the disassembled separator. (c) SEM image of the 15% SnO_2/Zn anode surface after 465 cycles and (d) the corresponding photos of the disassembled separator.

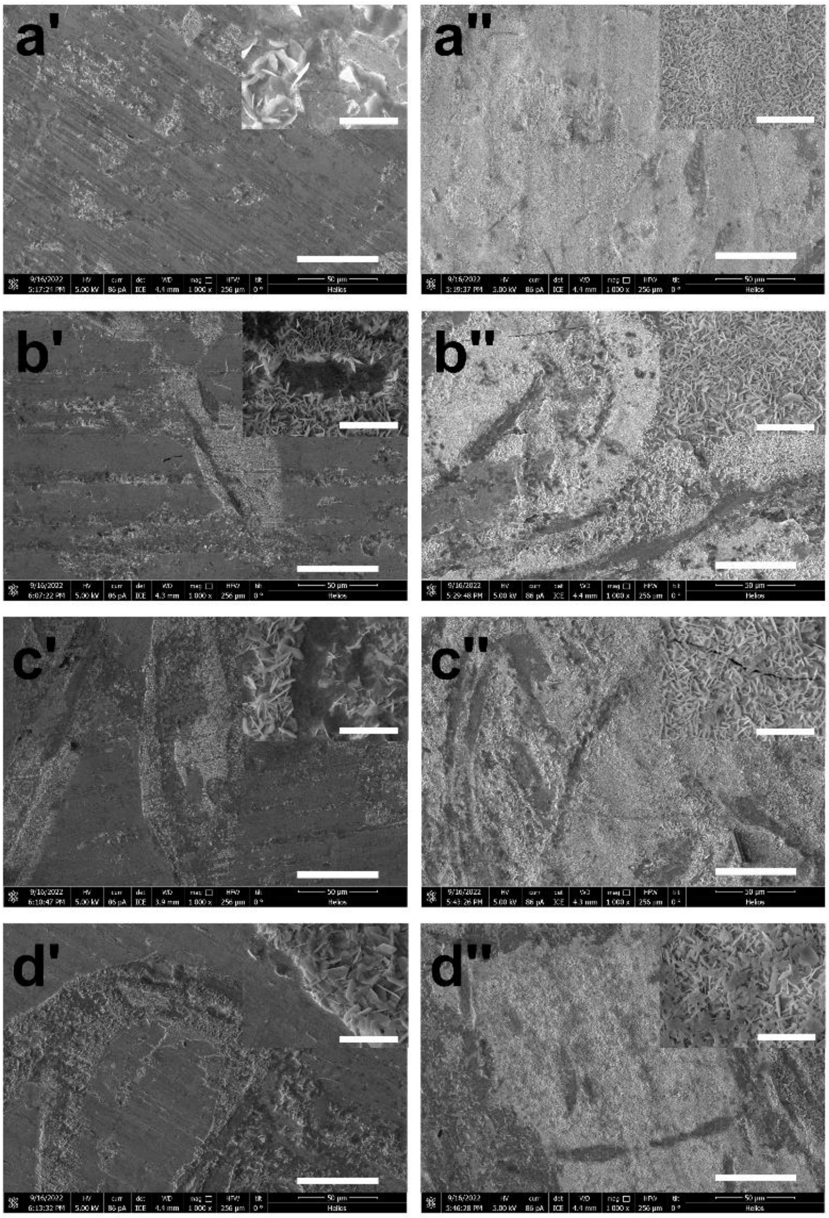

Fig. S14. SEM images of (a’-d’) bare Zn and (a’’-d’’) SnO_2/Zn electrodes after plating different amount of Zn: (a’, a’’) 0.01 mAh cm^{-2} at 0.1 mA cm^{-2}; (b’,b’’) 0.05 mAh cm^{-2} at 0.1 mA cm^{-2}; (c’, c’’) 0.1 mAh cm^{-2} at 1 mA cm^{-2}; (d’, d’’) 0.5 mAh cm^{-2} at 1 mA cm^{-2}. Scale bar: 50 μm. The insets are the corresponding enlarged images and their scale bar is 5 μm.

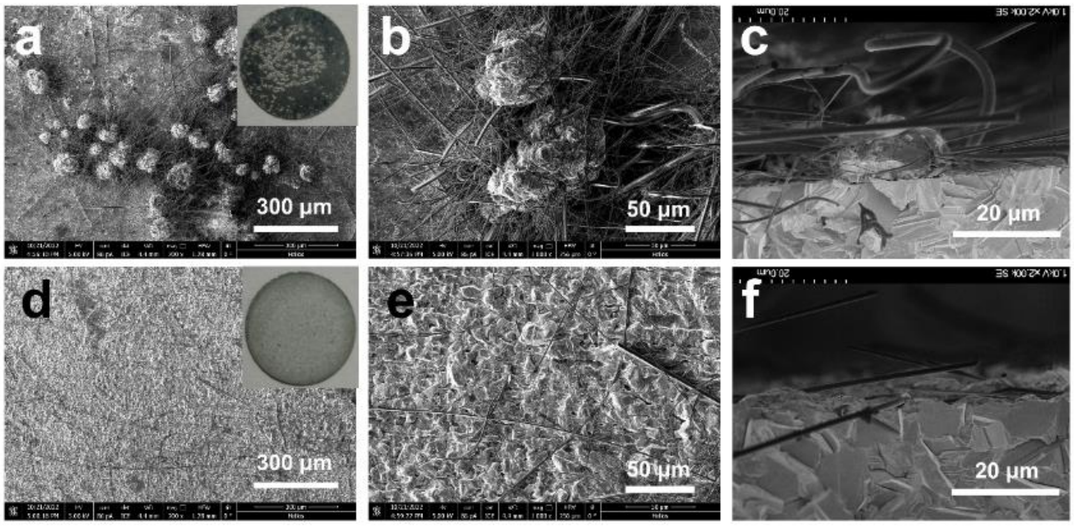

Fig. S15. SEM images of (a-c) bare Zn and (d-f) SnO_2/Zn electrodes at different magnifications and corresponding cross-sectional images after plating Zn for 1 mAh cm^{-2} at 1 mA cm^{-2}.

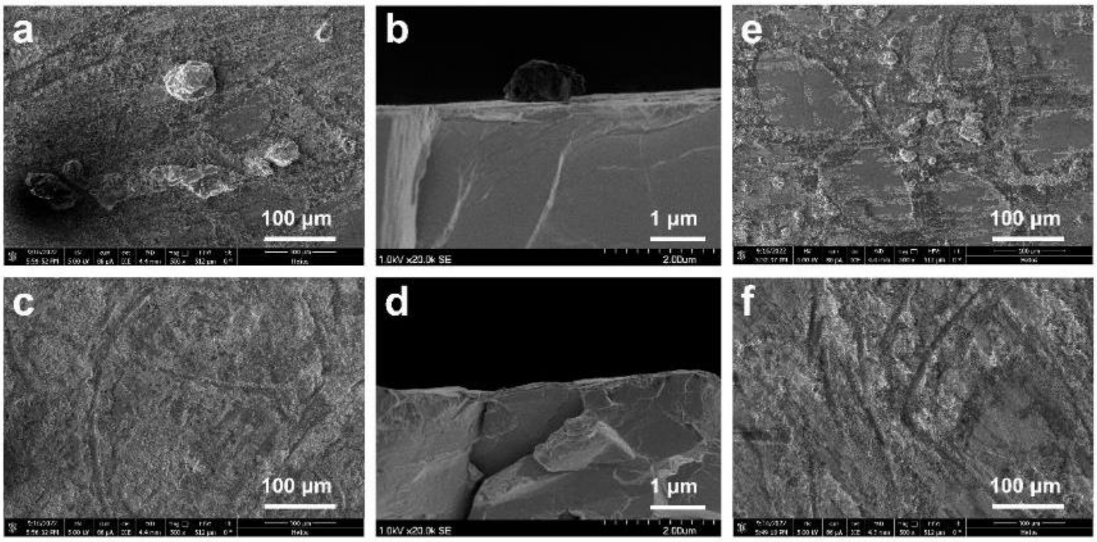

Fig. S16. SEM images of the anode surface on (a, b) bare Zn and (c, d) SnO_2/Zn, and the cathode surface on (e) bare Zn and (f) SnO_2/Zn after 20 cycles at 8 mA cm^{-2} and 0.4 mAh cm^{-2}.

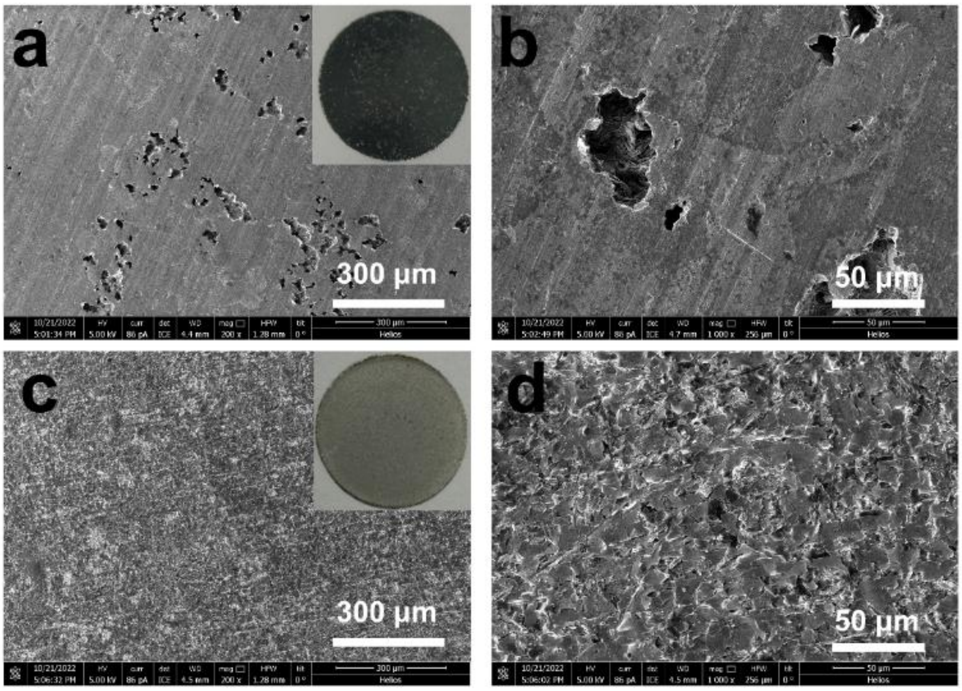

Fig. S17. SEM images of (a, b) bare Zn and (c, d) SnO_2/Zn electrodes after stripping Zn for 1 mAh cm^{-2} at 1 mA cm^{-2}.

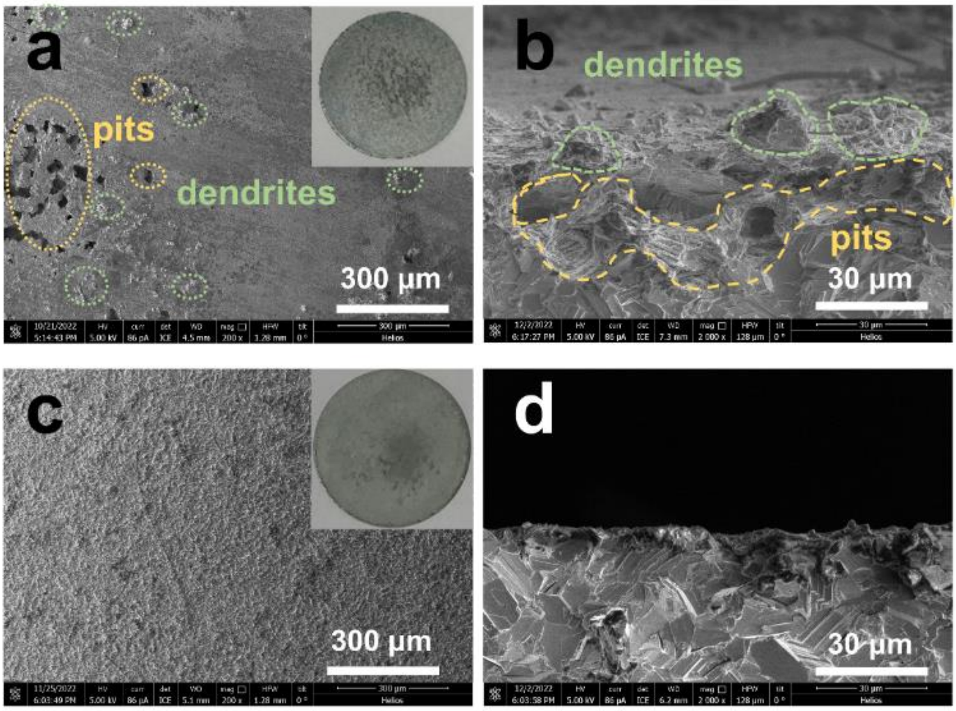

Fig. S18. (a and b) SEM images of (a) the bare Zn cathode surface after 20 cycles at 1 mA cm^{-2} and 1 mAh cm^{-2} and (b) the corresponding cross-sectional image. (c and d) SEM images of (c) the SnO_2/Zn cathode surface after 700 cycles at 1 mA cm^{-2} and 1 mAh cm^{-2} and (d) the corresponding cross-sectional image.

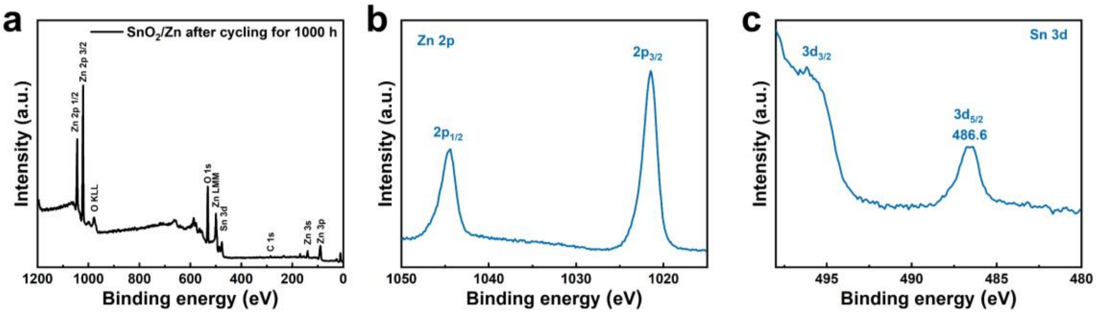

Fig. S19. (a) XPS survey spectrum and high resolution scan of (b) Zn 2p and (c) Sn 3d of the SnO_2/Zn after cycling for 1000 h.

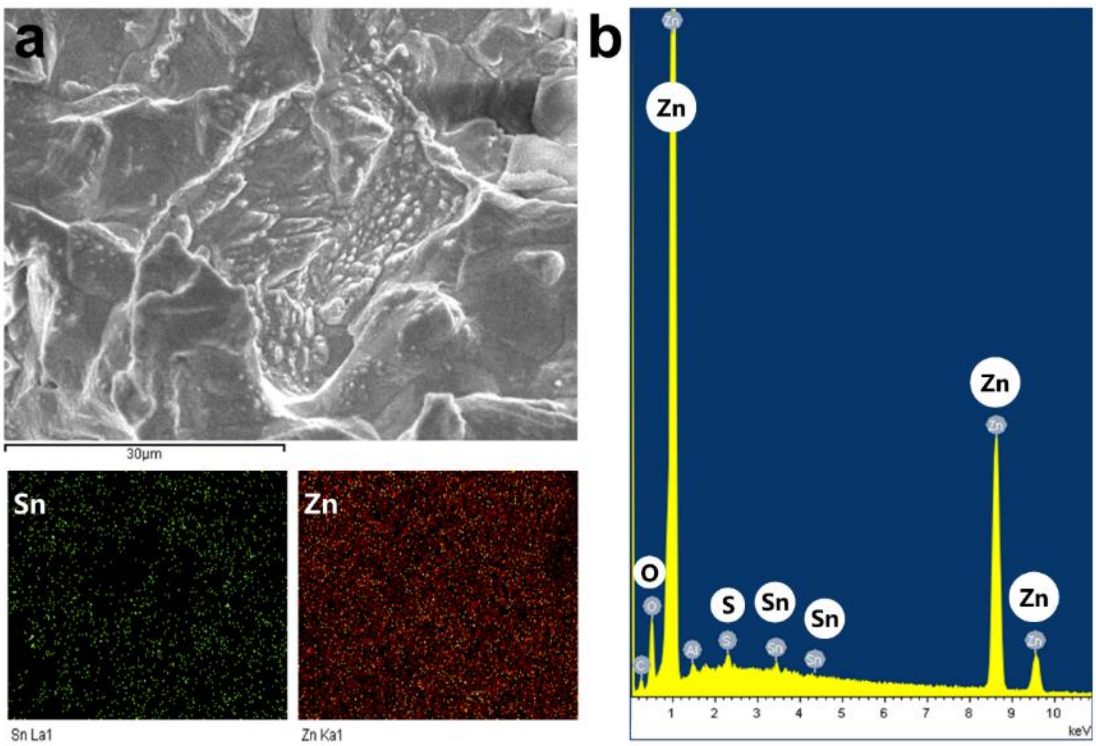

Fig. S20. (a) SEM image, elemental mappings and (b) the X-ray energy spectrum of the SnO_2/Zn after cycling for 1000 h.

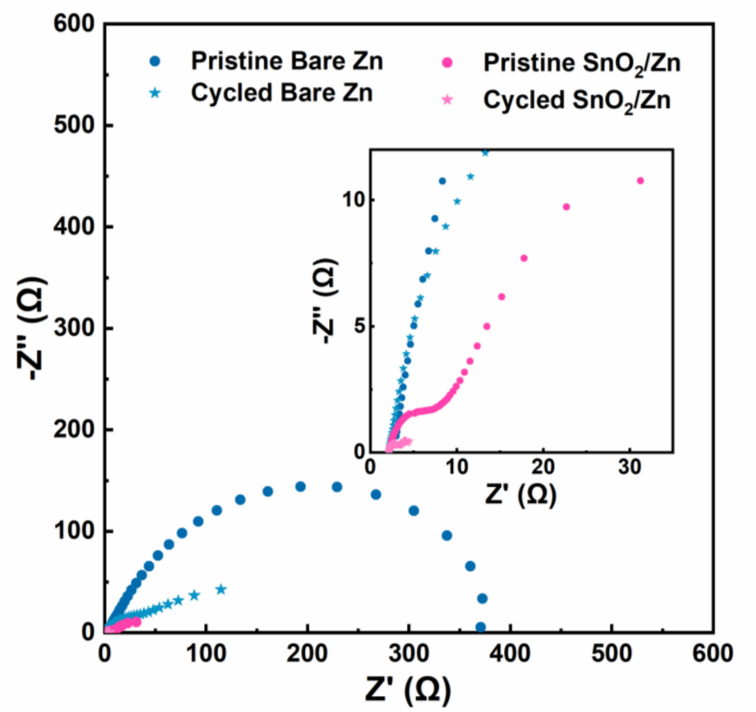

Fig. S21. EIS spectra (Nyquist plots) of bare Zn and SnO_2/Zn symmetrical cells before and after 200 cycles at 10 mA cm^{-2} and 1 mAh cm^{-2}

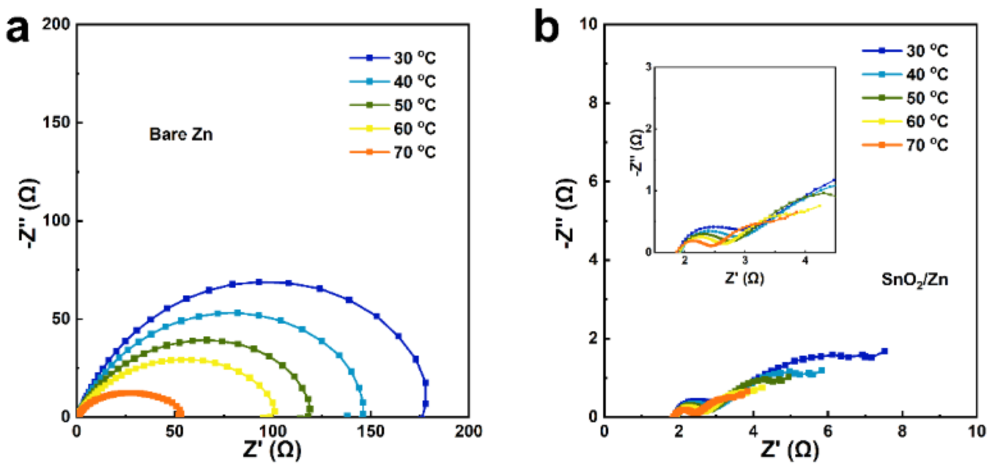

Fig. S22. EIS spectra (Nyquist plots) of Zn symmetrical cells without and with a SnO_2 layer at different temperatures

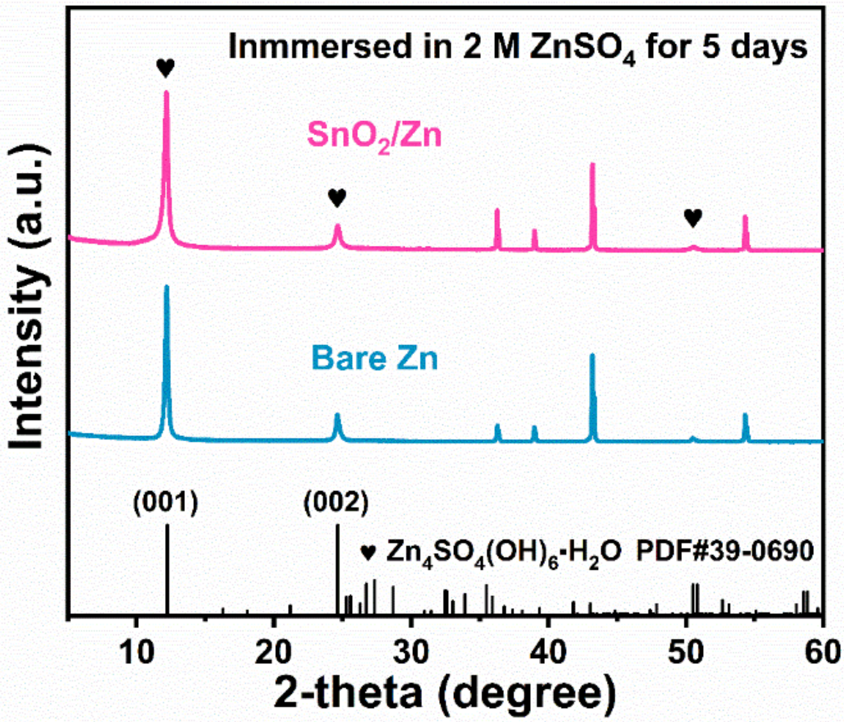

Fig. S23. XRD patterns of the Zn electrodes with or without the SnO_2 layer after immersing in 2 M $ZnSO_4$ electrolytes for 5 days

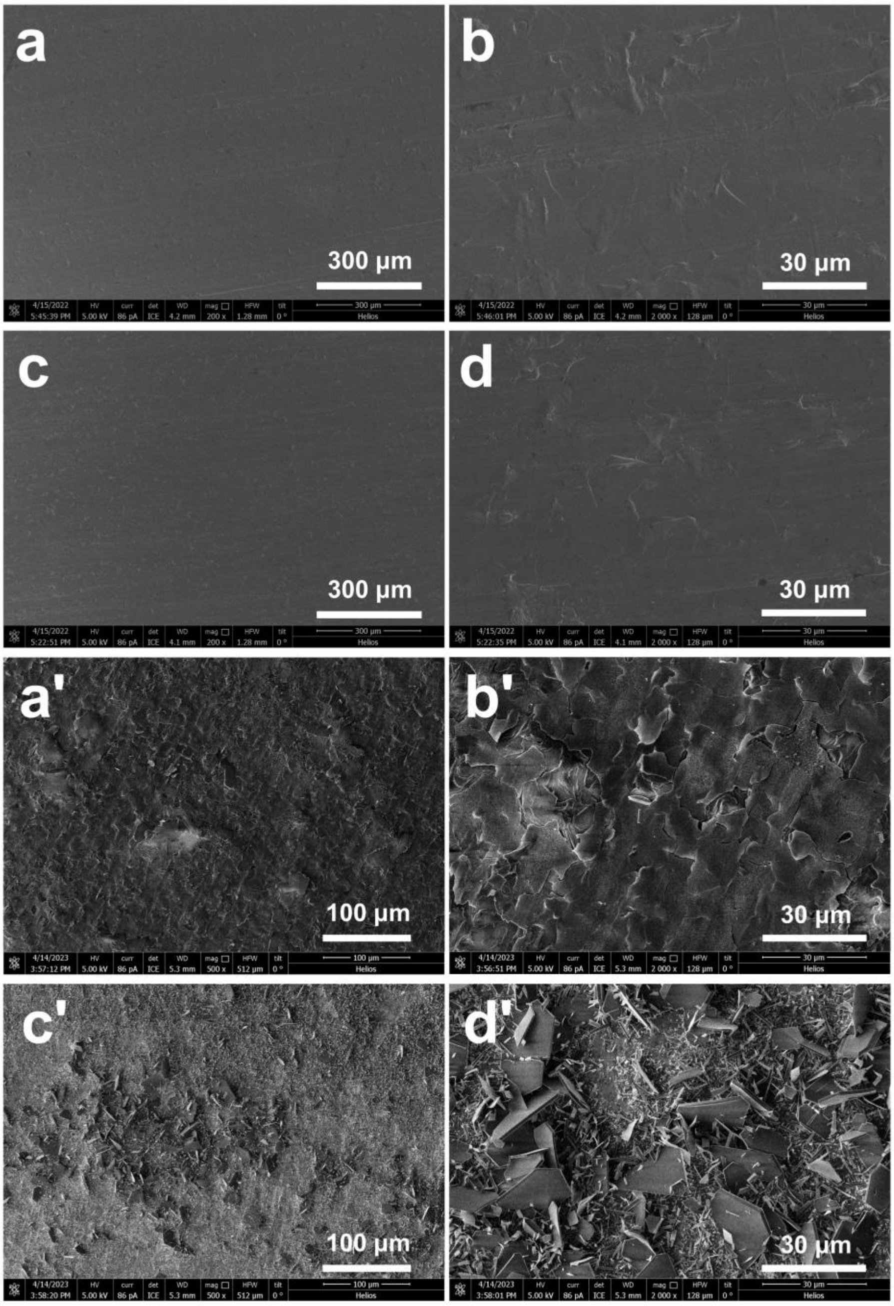

Fig. S24. SEM images of the Zn electrodes with (a, a’, b, b’) or without (c, c’, d, d’) the SnO_2 layer before (a-d) and after (a’-d’) immersing in 2 M $ZnSO_4$ electrolytes for 5 days.

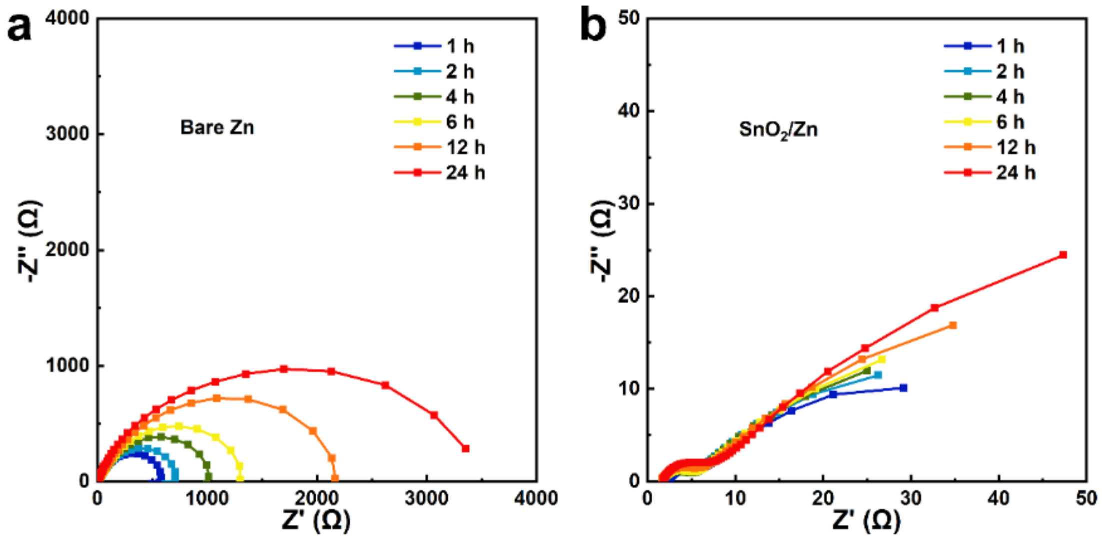

Fig. S25. Time-dependent EIS results of the Zn symmetrical cells without and with a SnO_2 layer.

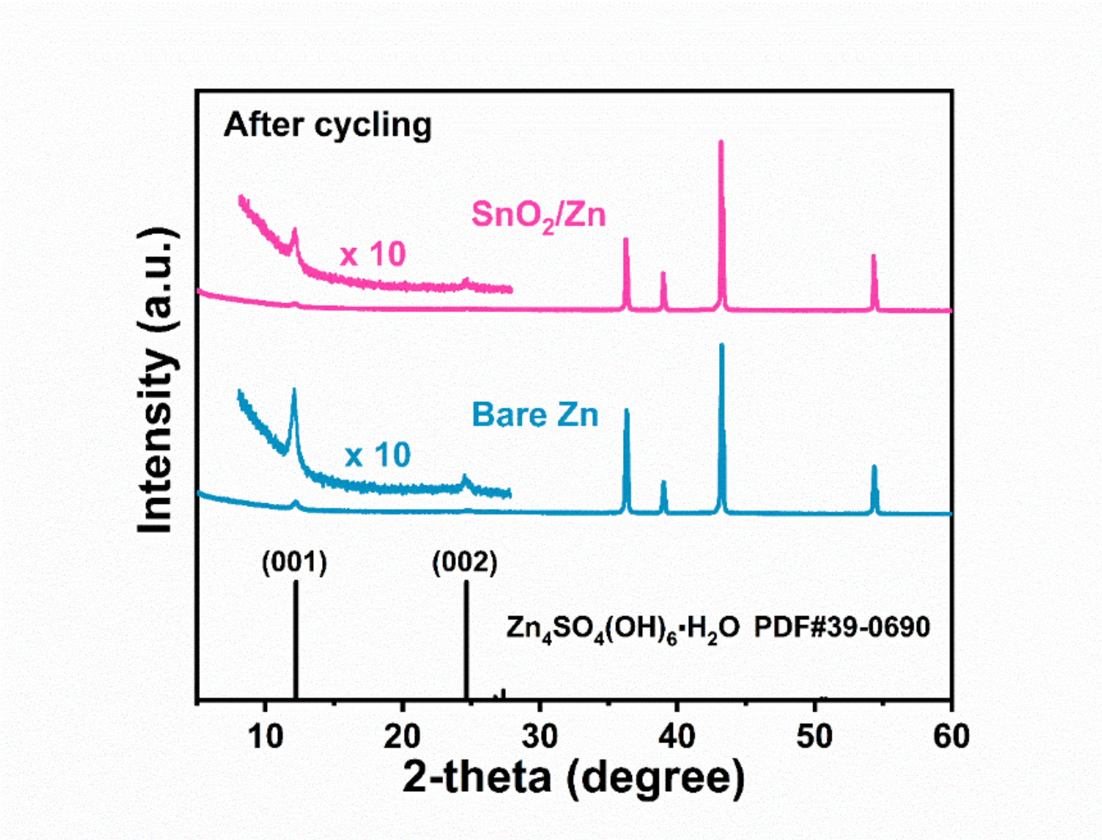

Fig. S26. XRD patterns of the Zn electrodes with or without the SnO_2 layer after 20 cycles

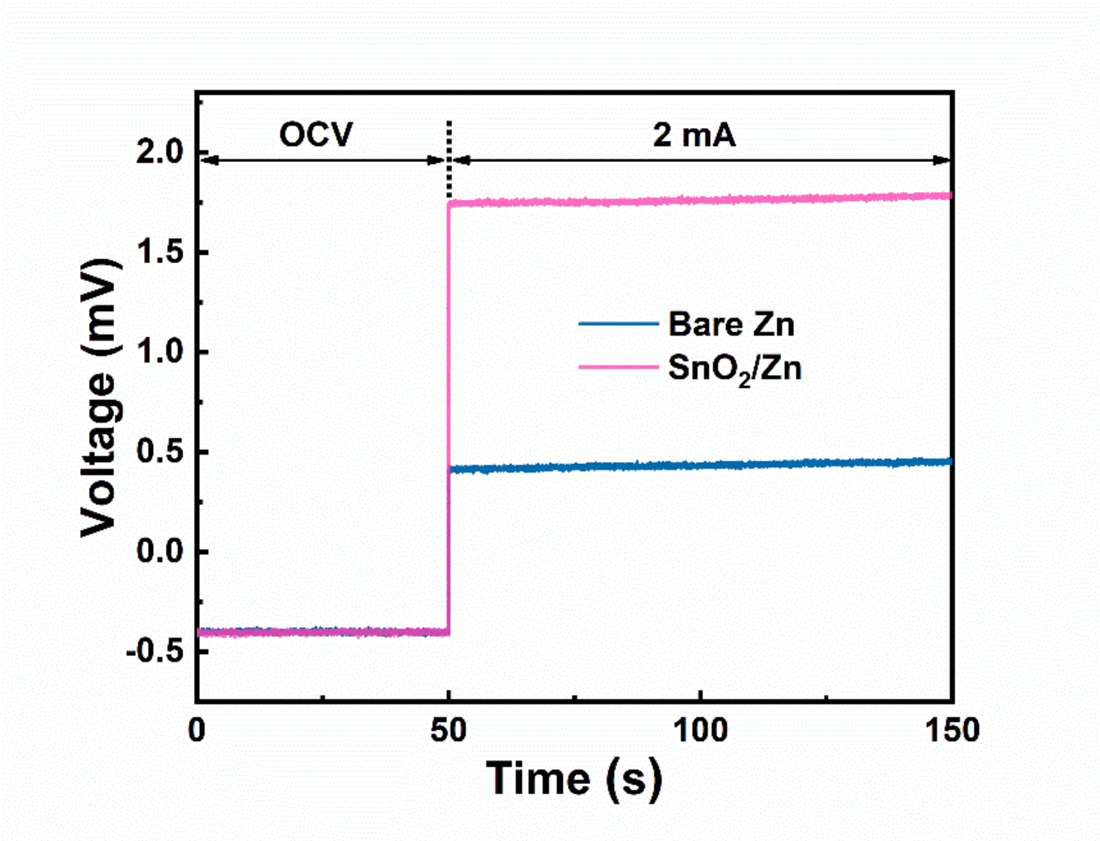

Fig. S27. The conductivity measurements of bare Zn and SnO_2/Zn electrodes. A direct current of 2 mA is applied at 50^{th} s, where the electrodes are individually sandwiched between two stainless steel blocking electrodes.

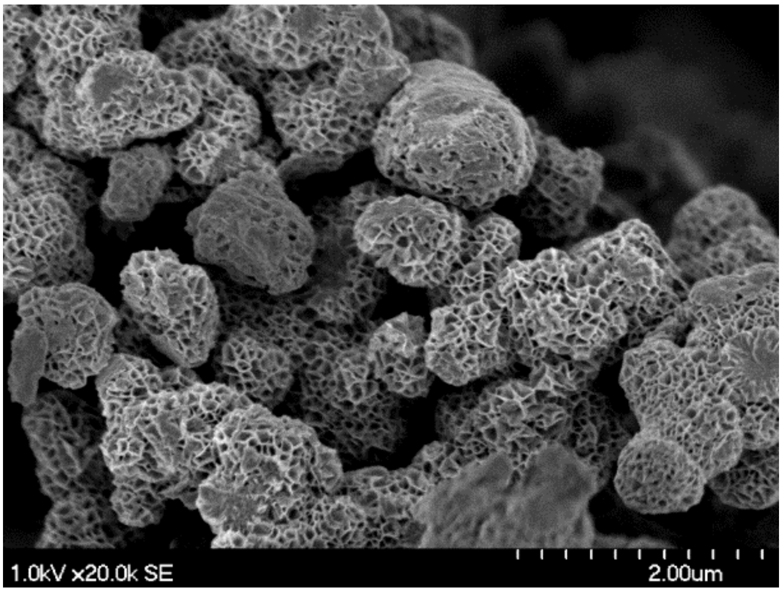

Fig. S28. SEM image of δ-MnO_2

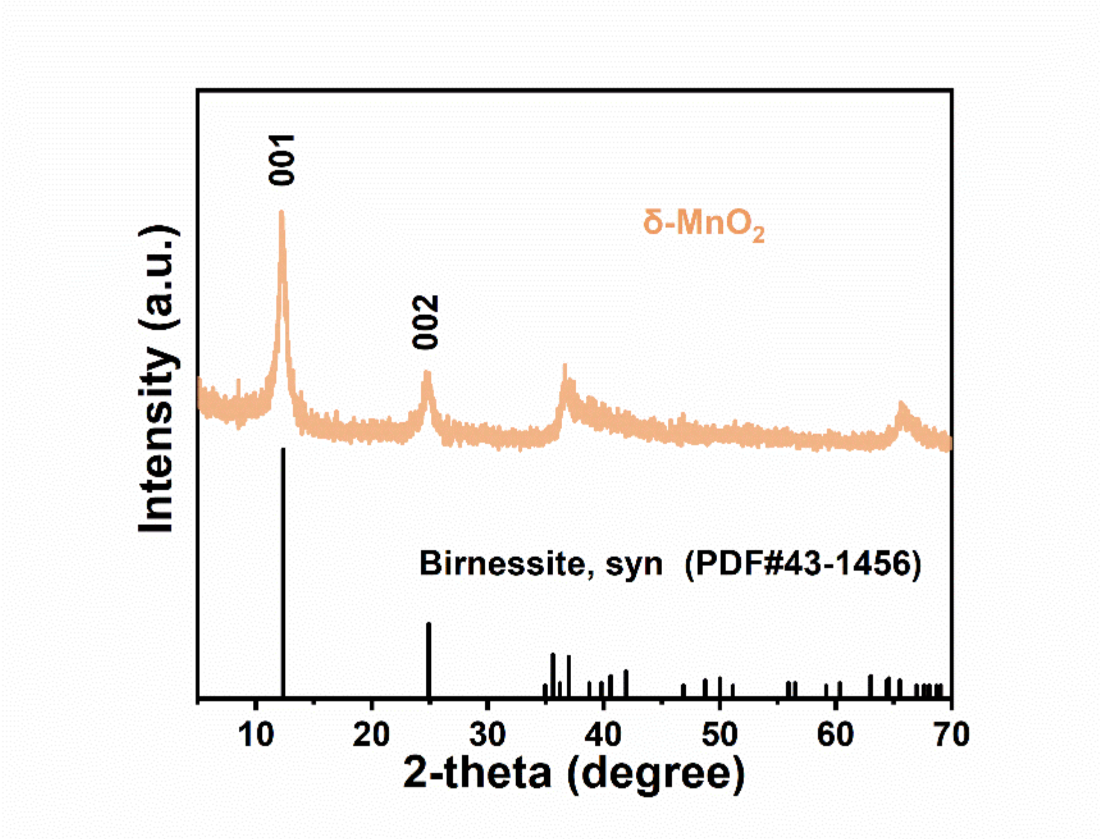

Fig. S29. XRD pattern of δ-MnO_2

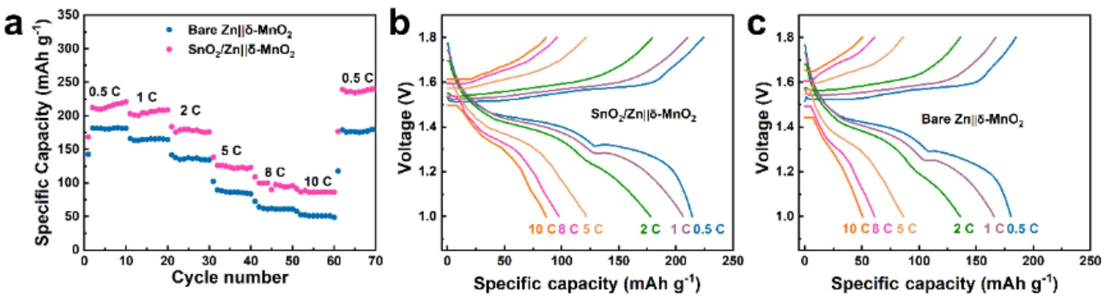

Fig. S30. (a) Rate performance of Zn||δ-MnO_2 full cells and the corresponding voltage profiles of (b) bare Zn||δ-MnO_2 and (c) SnO_2/Zn||δ-MnO_2 full cells at different current densities from 0.5 C to 10 C.

Table S1. The Inductively Coupled Plasma Mass Spectrometry (ICP-MS) results of the 2 M $ZnSO_4$ electrolyte (5 mL) obtained after different treatments

Element	Treatment	Content (µg/mL)
Sn	Black sample^{T1}	0.000001
Sn	Ultrasound for 5 min ^{T2}	0.0058
Sn	Immersing for 1 day ^{T2}	0.00045
Sn	Immersing for 3 days ^{T2}	0.0028
Sn	Immersing for 5 days ^{T2}	0.0036
Sn	60 cycles and 15 days rest ^{T3}	0.011 (*i.e.,* 0.055 µg)

^{T1}: original 2 M $ZnSO_4$ electrolyte (5 mL) without other treatment.

^{T2}: the 2 M $ZnSO_4$ electrolyte (5 mL) with 5 disks SnO_2/Zn electrodes (Φ 12 mm)

^{T3}: the SnO_2/Zn symmetrical cell was disassembled and fully immersed in the 2 M $ZnSO_4$ electrolyte (5 mL) after cycling for 60 times at 1 mA cm^{-2} and 1 mAh cm^{-2} and resting for 15 days. The 0.011 µg/mL Sn means the dissolved Sn in the SnO_2/Zn symmetrical cell is 0.055 µg.

Table S2. Comparison of the SnO_2/Zn anode with those of the reported Zn anodes at the current density of 2 mA cm^{-2} and area capacity of 1 mAh cm^{-2}

Design strategies for stable Zn anodes	Voltage polarization(mV)	CE	Cycle number	Reference
SnO_2 layer	**28.1**	**99.3%**	**2000**	**This work**
3D SS-CZ7	49.5	98.5%	470	[8]
DMA electrolyte additive	124.5	98.7%	250	[9]
ZnTe@Zn	75.8	99.16%	300	[14]
Zn-Mont	80.4	99.7%	1000	[37]
NCLZn	50	99.0%	700	[38]
Zn/Bi	54	99.6%	1000	[39]
502 glue layer	111.2	99.74%	200	[40]
PFSA layer	75	99.5%	600	[41]
h-Zn	45.4	99.57%	1200	[42]
CF separator	60	97.52%	200	[43]
MOF/rGO Janus Separator	140	99.2%	310	[44]

Table S3. Summary and comparison of recent protective layers with nanometer thickness or oxide materials for stable Zn anodes[S1-S5]

Protective layer of Zn anode	Synthesis method	Thickness	Asymmetrical cells			Symmetric cells			Reference
			Voltage polarization (mV)	Cycle number (C1, C2)[a]	CE	(C1, C2)[a]	Overpotential (mV)	Lifespan (h)	
SnO_2	**Spin-coating**	**~100 nm**	**28.1**	**2000 (2-1)**	**99.30%**	**0.5-0.5 1-1 5-1 8-4 30-1 10-10**	**10 10 35 40 90 53**	**3900 950 850 800 300 200**	**This work**
MTSi-Hedp	Dip-coating	~264 nm	-	-	-	1-0.5 1-1	30 28	2000 1250	[6]
HsGDY	In-situ growth	~490 nm	-	-	-	2--	60	2400	[11]
PA6/Zn(TfO)$_2$/LDH	Liquid self-assembly	~200 nm	-	-	-	0.5-0.5	30	1450	[15]
NGO	Langmuir-Blodgett method	~120 nm	-	-	-	1-1 5-5	17 48	1200 300	[21]
BN	Magnetron sputtering	~100 nm	74.3	150 (1-1)	99.3%	1-1 5-2.5	45 65	3000 1600	[23]
Al_2O_3	ALD	~10 nm	-	-	-	1-1	18	500	[24]
L-ZMF	Radio frequency sputtering	~25 nm	-	-	-	1-1	24	500	[25]
ILG	Spin-coating	~500 nm	~230	100 (0.1-0.1)	-	0.1-0.1 0.5-1.8	50 80	1000 400	[26]
Cu	Thermal evaporation	~300 nm	- ~95 -	700 (1-1) 3000 (10-1) 600 (10-3)	99.4% 99.7% 99.6%	1-1 5-2	38 70	5000 1500	[27]
SnO_2	ALD	~10 nm	-	-	-	0.25-0.05	10	300	[31]
PFSA	Coating	~500 nm	75	200 (2-1)	99.5%	1-1	20	800	[41]
SEI	Electrochemically pre-	~500 nm	52	200 (1-1)	99.5%	1--	50	2500	[49]

	cycling					5-- 10-5	60 120	600 450	
PS	Chemical reaction	~6.7 nm	-	-	-	1-0.5	40	1000	[51]
TiO_2	Atomic layer deposition (ALD)	~8 nm	-	-	-	1-1	25	150	[53]
Alucone	Molecular layer deposition	~12 nm	42.3	80 (0.5-0.5)	98.6%	3-1	52	780	[54]
CCF	Chemical conversion	~320 nm	49	120 (1.13-0.57)	99.1%	4.4-1.1	60	1200	[55]
β-PVDF	Spin-coating	~200 nm	-	-	-	0.25-0.05 1.5-0.3	40 49	2000 100	[56]
COF	Dip-coating and self-assembly	20-100 nm	~60	500 (4-1)	99.95%	1-1	27	400	[57]
FCOF	Pulling	~100 nm	293 210	320 (80-1) 250 (40-2)	97.2% 97.3%	5-1 40-1	60 200	1700 450	[58]
3D-COOH–COF	In-situ growth and post-synthetic modification	~150 nm	104	1000 (1-1)	99.5 %	1-1 3-1	40 50	2000 1200	[59]
PIM	Casting	~300 nm	50	~380 (3-3)	99.6%	0.5-0.5 5-5	30 62	1700 485	[60]
Al-ZnO (AZO)	Magnetron sputtering	~400 nm	69	100 (1-0.5)	99.51%	10-2 10-4.69	51 60	600 200	[61]
Passivation layer (Zn@Mn)	Chemical passivation	~65 nm	-	-	-	1-1 5-5	47 70	4000 85	[62]
$AgZn_3$	Plasma sputtering	~570 nm	55	375 (1-1)	-	1-1 4-2	32 39	1150 540	[63]
pi	Spin coating	~570 nm	-	1000 (4--)	99.5%	4-2	25	300	[64]
SIR	Dripping	~360 nm	45	1000 (1-1)	99.7%	2-2 10-10	40 58	3500 2000	[65]
CCF-K	Radiofrequency	~200 nm	-	4693 (1-1)	99.57%	1-1	21	10000	[66]

	plasma-assisted thermal evaporation								
MoS_2	Electrodeposition	~40 nm	-	-	-	2.5-0.416	60	175	[S1]
TpPa-SO_3H	Interfacial reaction	~100 nm	-	1000 (1--)	99%	-	-	-	[S2]
Fe_2O_3	ALD	-	-	-	-	0.1-0.05 1-1	20 24	1000 300	[S3]
m-TiO_2	Blade-coating	~20 µm	57	200 (4.4-1.1)	98.95%	(4.4-1.1)	37	500	[S4]
SiO_2	Coating	~20 µm	-	-	-	0.5-0.25 1-0.5	25 50	2000 1000	[S5]
ZnO	liquid-phase synthesis	~5 µm	45	300 (2-0.5)	99.55%	5-1.25	43	500	[12]
F-TiO_2	Slurry-pasting	~20 µm	-	-	-	1-1	25	460	[45]
CeO_2	Scraping	~10 µm	108	180 (2-1)	99.8%	0.5-0.25 5-2.5	60 80	1300 1300	[17]
Nb_2O_5	Spin coating	100 µm	72	100 (1-0.5)	98.01%	0.25-0.125 1-0.5	40 44	1000 1000	[20]
ZrO_2	Castig	~4 µm	72	70 (1-1)	95.5%	0.25-0.125 5-1	38 32	3800 2100	[16]
Sc_2O_3	Castig	0.65 mg cm^{-2}	64	260 (1.13-0.56)	99.85%	1-1	40	200	[70]

[a] (C1, C2): current density (mA cm^{-2}) and area capacity (mAh cm^{-2}).

Table S4. Summary of the performance of full cells with MnO_2 as cathodes and Zn as anodes (1C=0.308 A g^{-1})

Anode	Cathode	Electrolyte	Woking voltage (V)	Current density	Capacity (mAh g^{-1})	Cycle number	Capacity retention	Reference
SnO_2/Zn	**δ-MnO_2**	**2 M $ZnSO_4$+0.1 M $MnSO_4$**	**1.0-1.8**	**2C 0.5C 1C**	**133.4 210 205**	**500 - -**	**96.9% - -**	**This work**
Zn	δ-MnO_2	1 M $ZnSO_4$	1.0-1.8	0.166 A g^{-1}	~198	-	-	[70]
Zn	δ-MnO_2	1 M $ZnSO_4$+0.1 M $MnSO_4$	1.0-1.8	0.1 A g^{-1}	170	-	-	[71]
Zn	δ-MnO_2	1 M $ZnSO_4$+0.1 M $MnSO_4$	1.0-1.8	0.1 A g^{-1}	133	-	-	[72]
Zn	δ-MnO_2	2 M $ZnSO_4$+0.1 M $MnSO_4$	1.0-1.8	0.1 A g^{-1}	194	-	-	[73]
Cu@Zn	β-MnO_2	3 M $ZnSO_4$+0.1 M $MnSO_4$	0.8-1.9	1 A g^{-1}	~115	500	~76%	[26]
SnO_2@Zn	α-MnO_2	3 M $Zn(CF_3SO_3)_2$	0.8-1.8	1 A g^{-1}	~117	1500 (500)	~32% (~68%)	[31]
Sc_2O_3-coated Zn	MnO_2	2 M $ZnSO_4$+0.1 M $MnSO_4$	0.8-1.8	0.5 A g^{-1}	216.1	50	~57%	[74]
BTO@Zn	MnO_2	2 M $ZnSO_4$+0.1 M $MnSO_4$	1.0-1.8	2 A g^{-1}	~112	300	67%	[75]

Zn/C_3N_4	MnO_2	2 M $ZnSO_4$	0.8-1.8	1 A g^{-1}	~132	500	94.1%	[76]
Zn@ZnSe	α-MnO_2	2 M $ZnSO_4$+0.1 M $MnSO_4$	1.0-1.8	2C	273	1800 (500)	~34% (~54%)	[77]
ZnO/C-Zn	α-MnO_2	2 M $ZnSO_4$+0.1 M $MnSO_4$	0.8-1.8	1 A g^{-1}	151	1000 (500)	~48.7% (~73%)	[78]

References

S1 S. Bhoyate, S. Mhin, J. E. Jeon, K. Park, J. Kim and W. Choi, *ACS Appl Mater Interfaces*, 2020, **12**, 27249-27257.

S2 J. Zhao, Y. P. Ying, G. L. Wang, K. D. Hu, Y. D. Yuan, H. L. Ye, Z. L. Liu, J. Y. Lee and D. Zhao, *Energy Storage Mater.*, 2022, **48**, 82-89.

S3 Z. Zeng, Y. Zeng, L. Sun, H. Mi, L. Deng, P. Zhang, X. Ren and Y. Li, *Nanoscale*, 2021, **13**, 12223-12232.

S4 X. Zhou, P. Cao, A. Wei, A. Zou, H. Ye, W. Liu, J. Tang and J. Yang, *ACS Appl Mater Interfaces*, 2021, **13**, 8181-8190.

S5 X. Han, H. T. Leng, Y. Qi, P. Yang, J. X. Qiu, B. Zheng, J. S. Wu, S. Li and F. W. Huo, *Chem. Eng. J.*, 2022, **431**, 133931.